Environmental Science Advances

ROYAL SOCIETY OF CHEMISTRY

PAPER

View Article Online
View Journal

Cite this: DOI: 10.1039/d6va00175k

Trophic transfer of polylactic acid microplastics induces multisystemic dysfunction in *Tenebrio molitor* and challenges the perceived safety of biodegradable plastics

Bruna de Oliveira Mendes,[ab] Wesley Rodrigues Soares,[bc] Rafaela Ribeiro de Brito,[bc] Aline Sueli de Lima Rodrigues,[bd] Ariane Guimarães,[b] Boscolli Barbosa Pereira,[e] Thiarlen Marinho da Luz[bc] and Guilherme Malafaia *[bcd]

The trophic transfer of microplastics (MPs) in terrestrial food webs, particularly involving biodegradable polymers such as polylactic acid (PLA), remains poorly understood. In this study, we simulated a detritivore-based experimental food chain to investigate the transfer of PLA-MPs from *Musca domestica* to *Tenebrio molitor* and the resulting ecotoxicological effects. *M. domestica* larvae were exposed to PLA-MPs incorporated into the rearing substrate (4.2 mg kg^{-1}), and the presence of MPs was confirmed in newly emerged adults. These adults were then offered as prey to *T. molitor* larvae for five days, with subsequent confirmation of trophic transfer of PLA-MPs. Indirect exposure led to pronounced behavioral alterations, including locomotor rigidity, exploratory hesitation, and heightened phototactic response, with metrics such as immobility time, direction reversals, and spatial recurrence emerging as key discriminators in multivariate analysis. Growth and developmental impairments were also evident, characterized by ontogenetic delay, reduced biomass gain, and shifts in metabolic conversion. At the biochemical level, exposure induced marked disruptions in energy reserves (reduced protein and carbohydrate levels and elevated triglycerides), intensified digestive enzyme activity, and a pronounced redox imbalance – evidenced by increased reactive oxygen species, malondialdehyde, and nitrite, along with decreased superoxide dismutase and catalase activity. Neurochemical dysfunctions were also observed, including alterations in dopamine and serotonin levels and changes in acetylcholinesterase activity. Furthermore, functional network analysis revealed connectivity losses, reduced topological resilience, and a reconfiguration of biochemical co-activity patterns in response to PLA-MP exposure. Finally, integrative modeling *via* sparse partial least squares discriminant analysis demonstrated clear segregation between experimental groups, consolidating the evidence for multisystemic effects induced by trophic PLA-MP transfer. Collectively, these findings expand our understanding of the ecotoxicological risks posed by biodegradable polymers in terrestrial ecosystems, challenging the perceived environmental safety of materials labeled as biodegradable.

Received 15th April 2026
Accepted 8th May 2026

DOI: 10.1039/d6va00175k

rsc.li/esadvances

Environmental significance

This study demonstrates that microplastics derived from polylactic acid, a material widely promoted as biodegradable and environmentally safe, can be transferred across a terrestrial food chain and induce coordinated multisystem dysfunction in a secondary consumer following indirect exposure. By integrating behavioral, biochemical, and network-level responses, the findings reveal that even a single trophic step is sufficient to disrupt energy metabolism, redox balance, neurochemistry, and functional system organization in *Tenebrio molitor*. These results challenge the assumption that biodegradable plastics pose minimal ecological risk under natural conditions and highlight the need to incorporate trophic pathways and sublethal systemic effects into environmental risk assessment frameworks for emerging materials.

[a]*Post-Graduation Program in Genetic and Biochemical, Federal University of Uberlândia, Santa Mônica Campus, Uberlândia, Minas Gerais, Brazil*

[b]*Laboratory of Toxicology Applied to the Environment, Goiano Federal Institute, Urutaí Campus, Rodovia Geraldo Silva Nascimento, 2,5 km, Zona Rural, Urutaí, Goiás, CEP: 75790-000, Brazil. E-mail: guilherme.malafaia@ifgoiano.edu.br; Tel: +55 64 3465 1995*

[c]*Post-Graduation Program in Biotechnology and Biodiversity, Goiano Federal Institute, Urutaí Campus, Urutaí, Goiás, Brazil*

[d]*Post-Graduation Program in Conservation of Cerrado Natural Resources, Goiano Federal Institute, Urutaí Campus, Urutaí, Goiás, Brazil*

[e]*Department of Environmental Health, Federal University of Uberlândia, Santa Mônica Campus, Uberlândia, Minas Gerais, Brazil*

1. Introduction

In recent decades, microplastics (MPs) have emerged as a pervasive and insidious threat to the integrity of global ecosystems, disrupting essential ecological functions and triggering adverse effects across multiple levels of biological organization.[1–3] Although initially associated with marine pollution, growing evidence indicates that MPs are also widely distributed in terrestrial environments, urban areas, and agroecosystems, where they can accumulate in soils, groundwater, and biota.[4–7] This ubiquity is particularly alarming, given that MPs have already been detected in remote locations, including high-altitude regions, isolated islands, and glaciers, revealing the diffuse and transboundary nature of this pollution.[8,9] Defined as plastic particles ranging from 1 μm to 5 mm in diameter,[10] MPs originate either from the fragmentation of larger plastic debris (secondary MPs) or from the intentional production and release of microscale plastic particles (primary MPs), such as those used in cosmetics, industrial abrasives, and synthetic fibers.[11] Their physicochemical properties – including low density, high resistance to degradation, and strong adsorption capacity for organic and inorganic contaminants – promote environmental persistence and mobility across ecological compartments, increasing their bioavailability and potential for bioaccumulation.[12] While a substantial body of literature has focused on the impacts of MPs on marine[13,14] and freshwater organisms,[15,16] the effects of this pollutant class in terrestrial ecosystems, particularly in the context of trophic transfer, remain poorly understood and frequently overlooked in risk assessments.

Among the polymers that constitute microplastics (MPs), polylactic acid (PLA) has emerged as a supposedly sustainable alternative to conventional petroleum-derived plastics.[17–19] Produced from renewable sources such as corn starch and possessing potential biodegradability, PLA has been widely incorporated into packaging, disposable utensils, and biomedical products.[20] However, its labeling as "biodegradable" has been increasingly questioned by the scientific community, as its efficient degradation requires specific conditions of temperature, humidity, pH, and the presence of thermophilic microorganisms – conditions typically found only in industrial composting systems.[21–23] In natural environments, such conditions are rarely met, rendering PLA environmentally persistent in many contexts. Previous studies have warned that PLA, when fragmented at the microscale, can generate environmentally active MPs[24] capable of disrupting soil microbiota,[25] altering physical and physicochemical properties of soils,[26] modulating physiological processes such as seed germination, plant growth, and nutrient translocation,[27,28] and being ingested by soil fauna.[29–31] Nevertheless, investigations into the ecological behavior and toxicological effects of PLA-MPs in terrestrial food webs remain scarce, particularly regarding their indirect transfer through the consumption of contaminated prey by invertebrate or vertebrate predators.

Saprophagous insects, such as fly larvae, play a critical ecological role in the decomposition of organic matter, facilitating nutrient cycling, contributing to humus formation, and acting as agents of bioremediation.[32] Moreover, these larvae are a key component of terrestrial trophic networks, serving as a food source for a wide range of organisms, including birds, reptiles, mammals, amphibians, and predatory arthropods.[33,34] Previous studies have shown that larvae reared on substrates contaminated with MPs are capable of ingesting and accumulating these particles in their tissues, as demonstrated in *Synthesiomyia nudiseta*,[35] *Hermetia illucens*,[36] and *Drosophila melanogaster*.[37,38] Additionally, evidence suggests that MPs can persist across developmental transitions, with newly emerged adults retaining detectable particles after larval exposure, indicating carry-over retention during metamorphosis and potential mobilization across ecological contexts.[39] Despite such findings, the ultimate fate of MPs when predators consume contaminated insects remains unclear, and the potential ecotoxicological consequences of this indirect exposure have yet to be thoroughly explored.

Although the body of literature on the trophic transfer of MPs has expanded in recent years, most studies remain focused on aquatic ecosystems, particularly planktonic interactions and predator–prey relationships involving invertebrates and fish.[40–44] Terrestrial trophic interactions – especially those involving detritivore-based food chains;[45] from soil to chicken gizzards *via* earthworms in the backyard garden, and Chae & Na;[46] from soils to *Vigna radiata* and then to *Achatina fulica* – remain underexplored, representing a critical knowledge gap in understanding exposure pathways and the systemic impacts associated with MP contamination in continental environments. The possibility that MPs, including those labeled as biodegradable, may be efficiently transferred across terrestrial trophic levels, accumulate in higher trophic organisms, or induce sublethal effects after a single predation event challenges the prevailing assumption of their environmental safety.

In light of this scenario, this study aimed to evaluate whether PLA-MPs can be transferred through a prey-mediated terrestrial trophic route and whether this indirect exposure induces ecotoxicological effects in the secondary consumer *Tenebrio molitor*. Specifically, we tested the hypothesis that PLA-MPs retained in newly emerged *Musca domestica* adults can be transferred to *T. molitor* larvae *via* contaminated prey ingestion, eliciting coordinated behavioral, biometric, biochemical, and functional disturbances in the predator. The selection of *M. domestica* is supported by its broad geographic distribution, high adaptability to diverse organic substrates, and well-documented sanitary, ecological, and forensic relevance,[47,48] while *T. molitor* serves as a widely adopted model organism for direct MP exposure studies,[49–54] given its omnivorous habits, ease of laboratory maintenance, and increasing significance in both human and animal food chains.[55–58] Ecotoxicological effects were assessed using a multisystemic panel of behavioral, biometric, and biochemical biomarkers, encompassing locomotor impairments, larval growth alterations, and biochemical responses related to oxidative stress, energy metabolism, and enzymatic integrity. Furthermore, we applied a combination of inferential and multivariate statistical approaches to investigate integrated response patterns and test the hypothesis that PLA-

MPs are effectively transferred through a single trophic step, eliciting coordinated disruptions across multiple physiological systems. We believe that this study represents a conceptual and methodological advancement in the ecotoxicology of biodegradable MPs by integrating trophic transfer and biological functionality within a terrestrial detritivore model.

2. Material and methods

2.1. Polylactic acid microplastics

The PLA-MPs used in this study were previously prepared from commercial PLA pellets (Sigma-Aldrich, product no. GF45989881), following the procedures described previously.[35] Briefly, the production process involved mechanical grinding of the pellets, followed by oil-in-water emulsification, solvent evaporation, centrifugation, and drying, yielding spherical particles with smooth surfaces. The emulsification step was performed by adding the organic phase dropwise to a 1% poly(vinyl alcohol) aqueous phase under continuous stirring at 1700 rpm, followed by solvent evaporation under magnetic stirring at 900 rpm for 80 min at room temperature (23–24 °C). After brief homogenization in an ultrasonic bath for 40 s, the particles were collected by centrifugation at 12 000 rpm for 1 min and dried at 35 °C. To enable tracking in later analyses, the MPs were stained with the fluorescent dye Nile Red, as described previously.[59] Prior physicochemical characterizations revealed a mean diameter of 15.18 ± 0.40 μm and Raman spectra with well-defined peaks (874.35 cm^{-1}, 1133 cm^{-1}, 1457.7 cm^{-1}, and 1769.9 cm^{-1}), consistent with the intact molecular structure of the polymer. Additionally, morphological analysis by scanning electron microscopy (SEM) confirmed the regularity of the particles obtained.[35]

2.2. Animals and experimental design

The assessment of potential trophic transfer began with the induction of oviposition and subsequent collection of *Musca domestica* larvae, followed by their exposure to a substrate contaminated with PLA-MPs. For this purpose, moistened wheat bran (60% moisture; 8 kg), free of PLA-MPs, was used as a feeding and oviposition attractant. The material was distributed in three rectangular containers (40 × 30 × 15 cm) and kept in shaded conditions within the experimental area of the Laboratory of Environmental Toxicology (LabTox) at the Federal Institute of Education, Science, and Technology of Goiás (IF Goiano) – Urutaí Campus, Brazil. The moisture of the containers was monitored and maintained by daily replenishment of evaporated water. After confirming visitation and active oviposition by *M. domestica*, the containers were kept undisturbed for three days to allow early larval development. They were then transferred to the laboratory, where taxonomic identification was performed based on previous morphological descriptions,[60,61] confirming the species as *M. domestica* (Diptera: Muscidae). Subsequently, third-instar larvae were collected, and 1800 individuals were allocated into six glass beakers containing 1 kg of wheat bran each (300 larvae per beaker). Three beakers were filled with PLA-free substrate, forming the Control-larvae-*M. domestica* group, while the other three received PLA-MPs incorporated into the substrate at a concentration of 4.2 mg kg^{-1}, comprising the PLA-larvae-*M. domestica* group. This concentration was selected as a conservative low-level exposure scenario, given previous reports showing that visible plastic items in organic composts can occur at levels of 2.38–180 mg kg^{-1} compost, with additional evidence for smaller plastic particles.[62] Thus, the concentration used here lies near the lower end of values reported for organic matrices capable of introducing plastic particles into terrestrial systems and was considered environmentally realistic and ecologically plausible. All beakers were incubated in a climate-controlled chamber at 28 °C ± 0.5 °C, with a relative humidity of 50% ± 5.5%, and a 12 hour light–dark photoperiod. Organisms were monitored until adult emergence. To enable efficient collection of newly emerged individuals, each beaker was fitted with a structure that directed adult flight into a separate compartment isolated from the substrate zone. This physical separation enabled the effective collection of adult flies, which was performed daily until the sixth day after emergence, at which point the insects were immediately euthanized by exposure to −20 °C.

Subsequently, two experimental groups were established using *T. molitor* larvae derived from breeding stocks maintained in the Terrestrial Organisms Bioterium of LabTox (IF Goiano – Urutaí Campus, Brazil). The groups were standardized concerning initial body mass (150.5 ± 0.003 mg; mean ± SD; CV = 2.2%) and developmental stage (15.38 ± 0.25 instar; mean ± SD; CV = 4.6%) to minimize the effects of ontogenetic variation on subsequent experimental responses. The Control group was fed exclusively with newly emerged adult flies from the Control-larvae-*M. domestica* group, while the PLA group received adults from the PLA-larvae-*M. domestica* group. Food provisioning was standardized across groups (unpaired *t*-test, $t = 1.613$, $p = 0.1453$), with each experimental unit, rather than each larva, receiving an average of 118.5 ± 1.76 mg of adult flies per day for five consecutive days. Each group consisted of five experimental units, each containing 10 larvae, for a total of 50 larvae per group. Therefore, the amount of food offered corresponded to approximately 11.85 mg of flies per larva per day, assuming equal access among larvae.

2.3. Accumulation and interspecies transfer of PLA-MPs

To confirm the ingestion of PLA-MPs by *M. domestica* larvae, their retention in newly emerged adults, and subsequent transfer to *T. molitor* larvae, individuals of both species were analyzed for the presence of microplastics. Quantification of PLA-MPs was performed following previously described protocols,[35,63] with methodological adaptations. For *M. domestica* adults, eight biological pools were formed per experimental group (Control-larvae-*M. domestica* and PLA-larvae-*M. domestica*), each consisting of five individuals ($n = 40$ adults/group). For *T. molitor*, eight larvae per group (Control or PLA) were randomly selected from the experimental replicates. All specimens were initially rinsed with 70% ethanol, then macerated and homogenized in conical microtubes using

a bead mill homogenizer with stainless steel beads (4350 rpm; seven 60 second cycles with 60 second intervals), containing 1 mL of 10% KOH solution. The contents of each tube were transferred to glass vials containing 20 mL of the same KOH solution, hermetically sealed, and incubated in a water bath at 60 °C for 5 days to digest the biological tissues. After digestion, the residues were filtered through cellulose nitrate membranes (0.45 μm pore size) under negative pressure, dried in an oven at 37 °C for 12 hours, and analyzed under an epifluorescence microscope. Only particles exhibiting yellow fluorescence, consistent with prior Nile Red staining, were counted as PLA-MPs. Results were expressed as the number of particles per milligram of fresh biomass (particles per milligram of fresh biomass, MPs per mg).

2.4. Toxicity biomarkers

2.4.1. Behavioral assessment. To investigate potential behavioral effects associated with the trophic transfer of PLA-MPs, *T. molitor* larvae were evaluated for locomotor activity and phototactic responses at the end of the experimental period. Sixteen individuals per experimental group ($n = 16$ larvae/group) were randomly selected from the five replicates. Behavioral assessments were divided into two distinct sections: (i) evaluation of exploratory activity in a dark environment and (ii) evaluation of the negative phototactic response, adapted from previously established protocols.[64,65] All tests were conducted in a climate-controlled experimental room (28 ± 1 °C; 60% relative humidity) with acoustic insulation and controlled lighting conditions. Each larva was individually placed in the center of a Petri dish (13.5 cm diameter; 1.5 cm rim) and recorded for 5 minutes in complete darkness (dark phase). A 100-lumen LED light source was then positioned directly above the dish, and larval behavior was recorded for an additional 5 minutes (light phase). Petri dishes were cleaned with 70% ethanol between trials to eliminate chemical residues or pheromones that could interfere with subsequent tests. While the first section (dark phase) was designed to quantify spontaneous exploratory patterns associated with baseline locomotor motivation and neutral-environment activity, the second section (light phase) aimed to assess negative phototactic behavior, a characteristic of *T. molitor*, by measuring changes in movement patterns in response to sudden light exposure.

Behavioral analysis was based on trajectory tracking.[66] One hundred frames were extracted from each video (5 minutes per animal), and the images were processed using Fiji software (version 2.14.0). The manual tracking plugin (plugins > tracking > manual tracking) was used to obtain two-dimensional position data (X and Y coordinates) for each individual over time. Coordinates, initially in pixels, were converted to centimeters, and the data were processed in R (version 4.3.2) using the tidyverse, readxl, and writexl packages. Various primary and derived behavioral metrics were calculated for each individual and each experimental phase (dark and light), accounting for both spatial and temporal aspects of movement. A detailed description of the metrics analyzed in this study is provided in Table S1 (see "SI").

2.4.2. Biometric assessment. At the end of the behavioral tests, fifteen *T. molitor* larvae from each experimental group were randomly selected across the five replicates for biometric evaluation. Each individual was weighed (fresh mass, in mg) and photographed under a stereomicroscope to obtain morphometric measurements of total body length (mm) and head capsule width (mm), which were used both to determine larval instar[67] and to calculate various morphometric indices. The following parameters were estimated: (i) cephalo-corporeal ratio (head capsule width/total body length), used to infer the proportional development of the cephalic region relative to body length; (ii) length-to-mass ratio (total body length/body mass), indicative of structural elongation relative to accumulated biomass; (iii) body density (body mass/total body length), reflecting the degree of somatic compactness; (iv) cephalic allometry index (CAI) (head capsule width/total body length), which expresses cephalic allometry relative to body dimensions; and (v) mass conversion index (MCI) (body mass/(head capsule width)^3), used as a volumetric proxy for somatic growth efficiency based on the estimated cephalic volume. Additionally, we calculated Δ body biomass (mg) as the difference between the initial and final body mass of the larvae to assess net biomass variation throughout the experimental period, serving as an integrated indicator of physiological condition and resource assimilation efficiency.

2.4.3. Biochemical assessment. To evaluate biochemical effects associated with the trophic transfer of PLA-MPs, twelve *T. molitor* larvae were randomly selected, weighed, and homogenized in PBS (pH 7.2) using a tissue disruptor, following procedures similar to those previously described.[35] The homogenates were centrifuged (15 000 rpm, 10 min, 4 °C), filtered (0.45 μm), and stored at −80 °C until analysis. The biomarkers assessed included digestive, redox/detoxification, neurochemical, and bioenergetic reserve parameters, as summarized in Table S2 (see "SI").

2.5. Statistical analyses

2.5.1. Pairwise comparisons and factorial model with repeated measures. To compare biometric and biochemical biomarkers between the experimental groups (Control and PLA), each variable was analyzed individually using pairwise statistical tests. Data normality was assessed using the Shapiro–Wilk test, and homogeneity of variances was evaluated with Levene's test. When both assumptions were met, an unpaired t-test was applied; otherwise, the non-parametric Mann–Whitney test was used. For each analysis, the corresponding t or U values and associated p-values were reported. Results were graphically represented using estimation plots, which highlighted the mean (or median) differences, 95% confidence intervals, and the distribution of individual observations. Parametric data were expressed as mean ± standard deviation (SD), while non-parametric data were presented as median and interquartile range (IQR).

For the behavioral variables, which were repeatedly recorded during the dark and light phases of the test, a two-way repeated measures ANOVA was performed using a stacked matching data

structure and assuming sphericity. This approach enabled testing the main effects of treatment (PLA × Control) and the experimental phase (light × dark), along with their interaction, while accounting for the dependency of successive measures within the same individual. Before the analysis, residuals were also tested for normality (Shapiro–Wilk test) and for homogeneity of variances (Mauchly's test for sphericity, complemented by graphical inspection). In cases of moderate violation of parametric assumptions, ANOVA was retained due to its relative robustness, particularly given the balanced sample sizes across groups. When necessary, corrections for sphericity violations (*e.g.*, Greenhouse-Geisser) were considered, though none were applied in this study because no critical violations were observed. All tests were conducted with a significance level of $\alpha = 0.05$, and F values and p-values were reported. All analyses were performed using GraphPad Prism software (v.10.2).

2.5.2. Multivariate analyses

2.5.2.1. Partial least squares discriminant analysis (PLS-DA) and principal component analysis (PCA). To identify multivariate patterns associated with PLA-MPs, behavioral (Section 2.4.1), biometric (Section 2.4.2), and biochemical (Section 2.4.3) biomarkers were submitted to partial least squares discriminant analysis (PLS-DA). Analyses were conducted in R software (version 4.4.3) using the mixOmics package, with biomarker sets from each axis used as predictors (in separate models) and the experimental group (Control × PLA) as the response variable. To identify the most influential variables in group separation, Variable Importance in Projection (VIP) scores were calculated from the latent component loadings of the PLS-DA models; variables with VIP scores greater than 1.0 were considered highly discriminative. Interpretation was supported by biplots, in which biomarker vectors were projected into the discriminant space defined by group centroids, facilitating visualization of individual variable contributions to multivariate separation.

For behavioral biomarkers, two independent PLS-DA models were constructed: one using only data from the dark phase and another using data from both the light and dark phases. This approach enabled the identification of the behavioral variables most responsible for group differentiation under distinct light conditions. Additionally, to assess which group exhibited greater light-induced behavioral shifts, a Principal Component Analysis (PCA) was applied to the combined behavioral dataset (encompassing both phases and groups). PCA was chosen due to its unsupervised nature, avoiding forced separation bias while enabling the evaluation of natural shifts in multivariate behavioral profiles. Group centroids for the dark and light phases were calculated in PCA space, and Euclidean distances between these centroids were estimated as a measure of light-induced behavioral change magnitude. Results were visualized *via* trajectory plots, and the proportion of variance explained by the first two principal components (PC1 and PC2) was computed and reported to support the interpretation of emerging patterns.

2.5.2.2. Network topology and structural robustness analysis of biochemical biomarkers. To evaluate systemic interactions among biochemical biomarkers and estimate changes in global functional organization between experimental groups (Control and PLA), a network-based topological analysis was performed using correlation matrices. Initially, data were standardized using z-scores, and Spearman correlations were calculated for all biomarker pairs using the rcorr() function from the Hmisc package (R version 4.4.3), yielding both correlation coefficients and p-values. Network construction was performed using the igraph package, considering only correlations with absolute magnitudes ≥0.3 ($|r| \geq 0.3$), regardless of statistical significance, to capture biologically relevant interactions. For each network (Control and PLA), structural metrics were calculated, including the number of nodes, the number of edges, the average degree, the density, the global transitivity, and the modularity (*via* the cluster_fast_greedy() function). A Systemic Complexity Index (SCI) was then computed, assigning differentiated weights to network metrics based on their functional relevance (density = 0.3; transitivity = 0.2; average degree = 0.4; modularity with negative weight = 0.1). Degree and betweenness centralities of individual biomarkers were also calculated and compared across groups to identify highly connected nodes (hubs) or those playing strategic roles in inter-module communication.

Additionally, the functional resilience of biochemical networks was assessed through a structural robustness analysis based on degree-directed attacks, using undirected weighted graphs to quantify network vulnerability to the systematic removal of the most connected vertices, thereby simulating perturbations in highly central biomarkers. At each iteration, the node with the highest degree was removed, and the size of the largest connected component (*i.e.*, the largest subgraph in which all vertices remain interconnected) was recalculated as a measure of functional network integrity. Co-occurrence networks were preconstructed using Spearman correlations, considering only statistically significant interactions ($p < 0.05$), and were generated using the igraph, tidygraph, and ggraph packages in the R environment (version 4.4.3). Resilience was expressed as a percolation curve, with the X-axis representing the cumulative proportion of removed biomarkers and the Y-axis representing the remaining size of the largest connected component.

2.5.2.3. Multivariate discrimination of functional biomarkers via sparse PLS-DA modeling. Finally, to discriminate *T. molitor* larvae fed with *M. domestica* adults previously exposed or not to PLA microplastics, we performed a sparse Partial Least Squares Discriminant Analysis (sPLS-DA) using the mixOmics package (version 6.24.0) in the R environment. Initially, all numerical variables ($n = 59$ biomarkers) were standardized using z-score transformation *via* the scale() function. A collinearity filter was then applied using the findCorrelation() function from the caret package with a cutoff of $r > 0.90$, resulting in the exclusion of 11 redundant variables and the retention of 48 independent biomarkers. The sPLS-DA model was fitted with two latent components (ncomp = 2), imposing sparsity through the keep $X = c(10, 10)$ parameter to select the 10 most discriminative variables per component, thereby avoiding overfitting and maximizing model interpretability. The proportion of variance explained by each component was obtained using the explained_variance()

function, based on the variance of the scores extracted from the fitted model. Model adequacy was further assessed by inspecting individual score distributions, the distance between group centroids, and the orientation of selected biomarker vectors in the discriminant space. Additionally, Variable Importance in Projection (VIP) scores were calculated using the vip() function to identify and rank the most relevant biomarkers in each component for distinguishing between groups. A hierarchical clustering analysis was then conducted on the VIP scores of both components using the pheatmap() function with Euclidean distance and complete linkage method, aiming to detect potential patterns of functional modularity and co-activation among the discriminant biomarkers.

3. Results

The ingestion and retention of PLA-MPs by *M. domestica* were initially confirmed by detecting fluorescent particles in newly emerged adults originating from the contaminated substrate, demonstrating not only larval ingestion but also stage-to-stage transfer of these particles into adulthood (Fig. 1A, C and D). Quantitatively, contaminated adult flies contained 125.6 ± 76.01 PLA particles per mg body biomass, whereas no fluorescent PLA-MPs were detected in control individuals. When these flies were used as food for *T. molitor*, they mediated the trophic transfer of PLA-MPs, as the particles were likewise detected in the predatory larvae – without any observed lethality during the experimental period – although at substantially lower concentrations than in the prey. Specifically, *T. molitor* larvae showed a mean recovered burden of 11.92 ± 4.78 PLA particles per mg body biomass, with a median value of 12.24 ± 1.69 PLA particles per mg body biomass (Fig. 1A). In addition to this lower particle burden, PLA-MPs recovered from *T. molitor* larvae exhibited reduced diameters compared with those detected in *M. domestica* adults (Fig. 1B, E and F). Conversely, behavioral analyses revealed significant functional alterations. The two-way repeated measures ANOVA indicated significant effects of

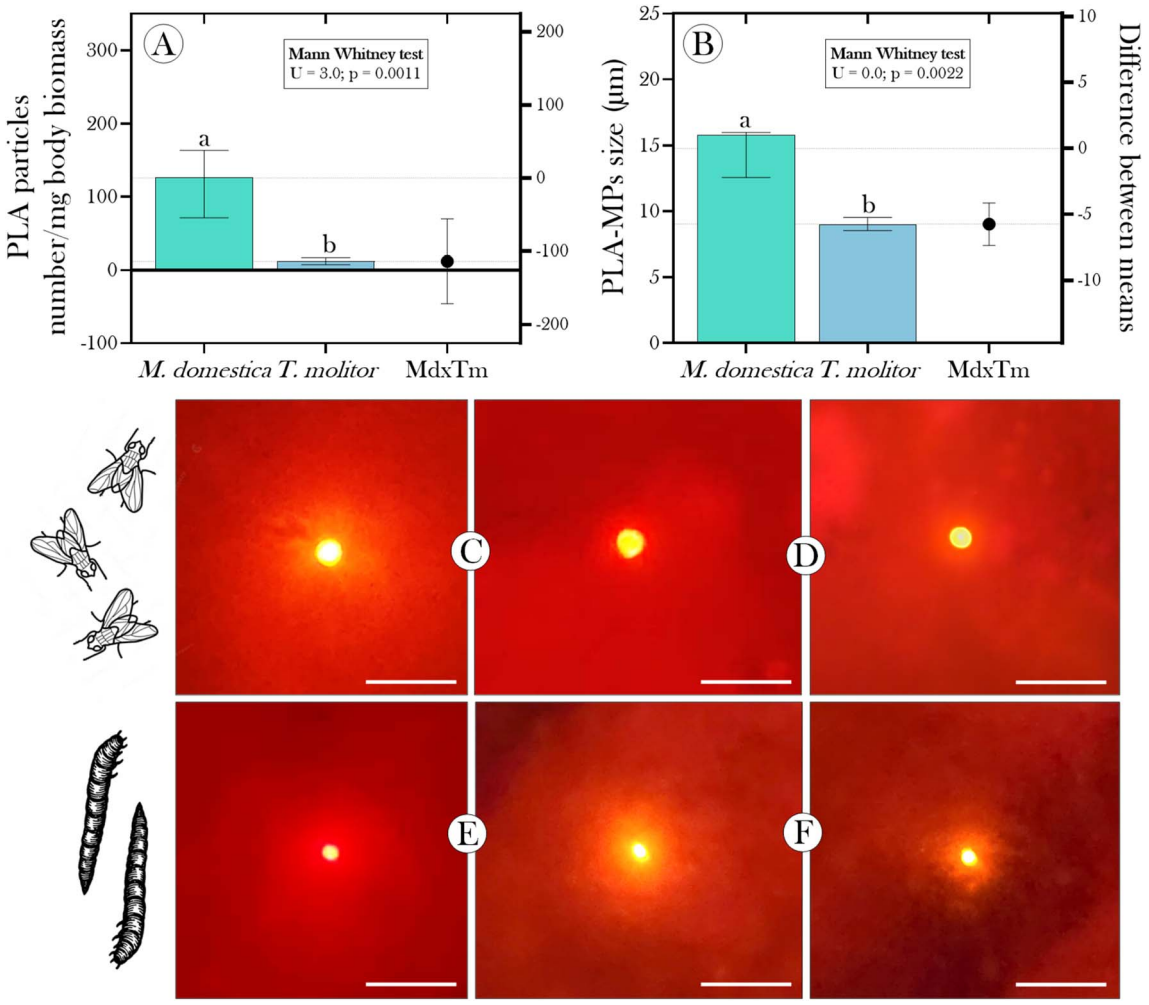

Fig. 1 Detection and quantification of polylactic acid microplastics (PLA-MPs) in an experimental prey-mediated transfer model [*Musca domestica* (Md) → *Tenebrio molitor* (Tm)] using Nile Red fluorescence. (A) Number of PLA-MP particles and (B) mean particle diameter (µm) detected in *M. domestica* adults and *T. molitor* larvae. Bars represent median ± interquartile range (non-parametric data), and the estimation plots display the difference between group medians with 95% confidence intervals. Mann–Whitney test results are shown at the top of each graph. (C–F) Representative epifluorescence micrographs showing PLA-MPs (in yellow) in (C and D) *M. domestica* adults and (E and F) *T. molitor* larvae. Scale bars: 50 µm. MP: microplastic; PLA-MP: polylactic acid microplastic.

both the interaction between experimental phase (dark and light) and treatment (Control *vs.* PLA), as well as of each factor independently, depending on the behavioral metric analyzed (Fig. S1 and S2, see "SI"). These findings were further supported by PLS-DA, which revealed a clear separation between the groups in both test phases, dark (Fig. 2A) and light (Fig. 2B), highlighting consistent alterations in locomotor activity patterns induced by indirect exposure to PLA-MPs.

Among the behavioral metrics, number of direction reversals (NDR), time spent immobile (TSI), and spatial recurrence index (SRI) stood out, all exhibiting VIP scores greater than 1.0 in both phases of the test, indicating high discriminative power (Fig. 2C and D). Exposed larvae showed a lower frequency of directional changes (NDR; Fig. S2C), increased immobility time (TSI; Fig. S1D), and higher spatial recurrence (SRI; Fig. S2A), suggesting a more rigid, hesitant, and less exploratory locomotor pattern. Still in the dark phase, exposed larvae also displayed significantly reduced spatial entropy (SE) and fractal complexity (FC) compared to controls (Fig. S2D and E), with VIP values exceeding 1.0, indicating more constrained, less complex movement trajectories. When exposed to light stimulation, PLA group larvae exhibited a 66.27% reduction in distance traveled (DT) compared to the control group (Fig. S1A), accompanied by a 52.6% increase in the Locomotor Irregularity Index (LII) (Fig. S2F), characterizing a more erratic, disorganized, and energetically inefficient locomotor pattern. Additionally, PCA, which integrated data from both the dark and light phases (with PC1 and PC2 explaining 45.32% and 22.82% of the total variance, respectively), revealed that both groups altered their behavior in response to light exposure, as evidenced by the displacement of behavioral centroids in multivariate space (Fig. 2E). However, while the control group exhibited only a modest shift between phases, the PLA group showed a substantial trajectory, with centroid displacement more than three times greater than that of the Control group.

In addition to behavioral disturbances, indirect exposure to PLA-MPs impaired key growth and developmental parameters in *T. molitor*, with pronounced alterations in morphometric biomarkers. Larvae fed with contaminated *M. domestica* exhibited a lower mean instar compared to the control group, whose individuals showed ontogenetic progression during the experiment (initial value: 15.38 ± 0.25; final: 16.08 ± 0.13) (Fig. S3A – see "SI"). This developmental delay was accompanied by reduced body biomass gain, reflected in the decrease of Δ body biomass (Fig. S3D) and, interestingly, by an approximate 17% increase in the Mass Conversion Index (MCI) relative to the control group (Fig. S3E), indicating a greater metabolic investment required to convert cephalic volume into body mass – possibly associated with imbalances in somatic growth. These three indicators-instar, biomass, and MCI-emerged as the main discriminative descriptors in the PLS-DA (Fig. S3J and K), playing a decisive role in the multivariate segregation between groups and reinforcing the hypothesis that the trophic transfer of PLA-MPs compromises fundamental aspects of ontogenetic performance. In contrast, we did not observe significant differences between groups for body density (BD), length-to-mass ratio (LTMR), cephalo-corporeal ratio (CCR), or cephalic allometry index (CAI) (Fig. S3F–I).

Exposed larvae exhibited reductions in total protein (TP) (Fig. S4A, see "SI") and total soluble carbohydrates (TSC) (Fig. S4C), indicating impairment of protein structure and readily mobilizable energy reserves. Conversely, triglyceride (TAG) levels were significantly elevated in the PLA group (Fig. S4B), which, together with reductions in the relative allocation of energy to proteins (RAETP; Fig. S4D) and carbohydrates (RAETSC; Fig. S4F), and an increase in lipid allocation (RAETAG; Fig. S4E), suggests a metabolic shift favoring lipid accumulation. This trend is corroborated by increases in the Lipid-to-Protein Index (LPI) (Fig. S4H) and decreases in the Rapid Energy Allocation Index (REAI) (Fig. S4G), indicating lower metabolic readiness for immediate energy use and greater emphasis on long-term energy storage. Although the Protein-to-Carbohydrate Index (PCI) (Fig. S4I) and the Bioenergetic Condition Index (BCI) (Fig. S4J) did not differ significantly between groups, the PLS-DA revealed a clear separation of bioenergetic profiles in multivariate space (Fig. S4K and L), indicating that the changes were sufficiently coordinated to discriminate the groups based on their metabolic signature.

Additionally, we observed distinct biochemical alterations between experimental groups, encompassing multiple functional axes. In the digestive axis, *T. molitor* larvae from the PLA group showed a significant increase in the activities of trypsin, chymotrypsin, lipase, and alkaline phosphatase (Fig. S5A–D, see "SI"), suggesting an upregulation of digestive enzyme activity and a possible adaptive response to stress. Within the redox axis, a pronounced oxidative imbalance was detected, marked by elevated levels of reactive oxygen species (ROS) and malondialdehyde (MDA) (Fig. S5E and F), along with a reduction in superoxide dismutase (SOD; −12.15%) and catalase activity (−45.94%) (Fig. S5G and H). Although no differences were found between groups for glutathione S-transferase (GST) activity (Fig. S6A, see "SI"), cytochrome P450-type oxidase activity was significantly higher in PLA-exposed larvae (Fig. S6B), indicating the induction of xenobiotic-metabolizing enzymes. Additionally, nitrosative stress was inferred from the increased levels of nitrite (NO_2^-) in the PLA group (Fig. S6C). In the neurochemical axis, there was a marked reduction in dopamine and 5-HT levels (Fig. S6D and E), contrasting with an approximate 60% increase in acetylcholinesterase (AChE) activity in the same individuals (Fig. S6F), suggesting potential cholinergic dysfunction.

A reorganization in the functional topology of correlation networks among the evaluated biomarkers further supported these systematized biochemical alterations. As shown in Fig. 3A and B, both networks (Control and PLA) contained 17 nodes, but differed in the total number of edges (84 *vs.* 77, respectively), indicating a loss of connectivity under PLA exposure. This difference was reflected in structural metrics, with reductions in density (0.618 → 0.566), average degree (9.88 → 9.06), and modularity (0.105 → 0.087), alongside a slight increase in transitivity (0.689 → 0.705), potentially indicating localized rearrangements in functional connectivity. Degree centrality analysis revealed a loss of connectivity in key biomarkers such

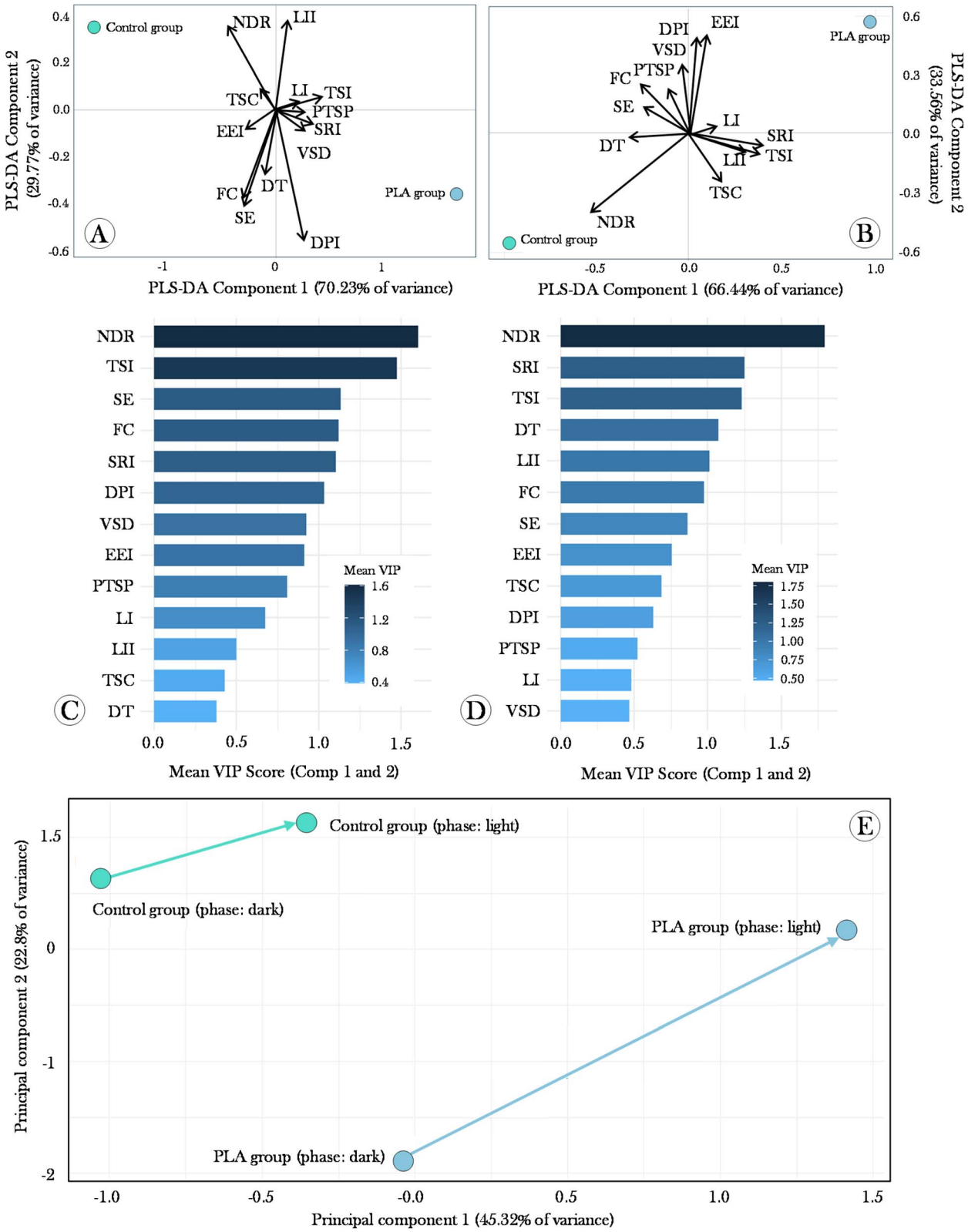

Fig. 2 Multivariate discrimination and behavioral feature importance in *Tenebrio molitor* larvae following trophic exposure to polylactic acid microplastics (PLA-MPs). (A and B) Discriminant maps generated by Partial Least Squares-Discriminant Analysis (PLS-DA) based on locomotor parameters recorded during the (A) baseline dark phase and (B) aversive light phase of the open field test. (C and D) Variable Importance in Projection (VIP) scores for each behavioral trait under the same respective phases, indicating their relative contribution to group discrimination. (E) Principal Component Analysis (PCA) score plot showing centroid trajectories between phases, evidencing a greater behavioral shift in the PLA-MP group. Abbreviations: DT, distance traveled; TSC, time spent in center; PTSP, percentage of time spent in the periphery; TSI, time spent immobile; VSD, velocity standard deviation; LI, linearity index; SRI, spatial recurrence index; DPI, directional persistence index; NDR, number of direction reversals; SE, spatial entropy; FC, fractal complexity; LII, locomotor irregularity index; EEI, efficient exploration index.

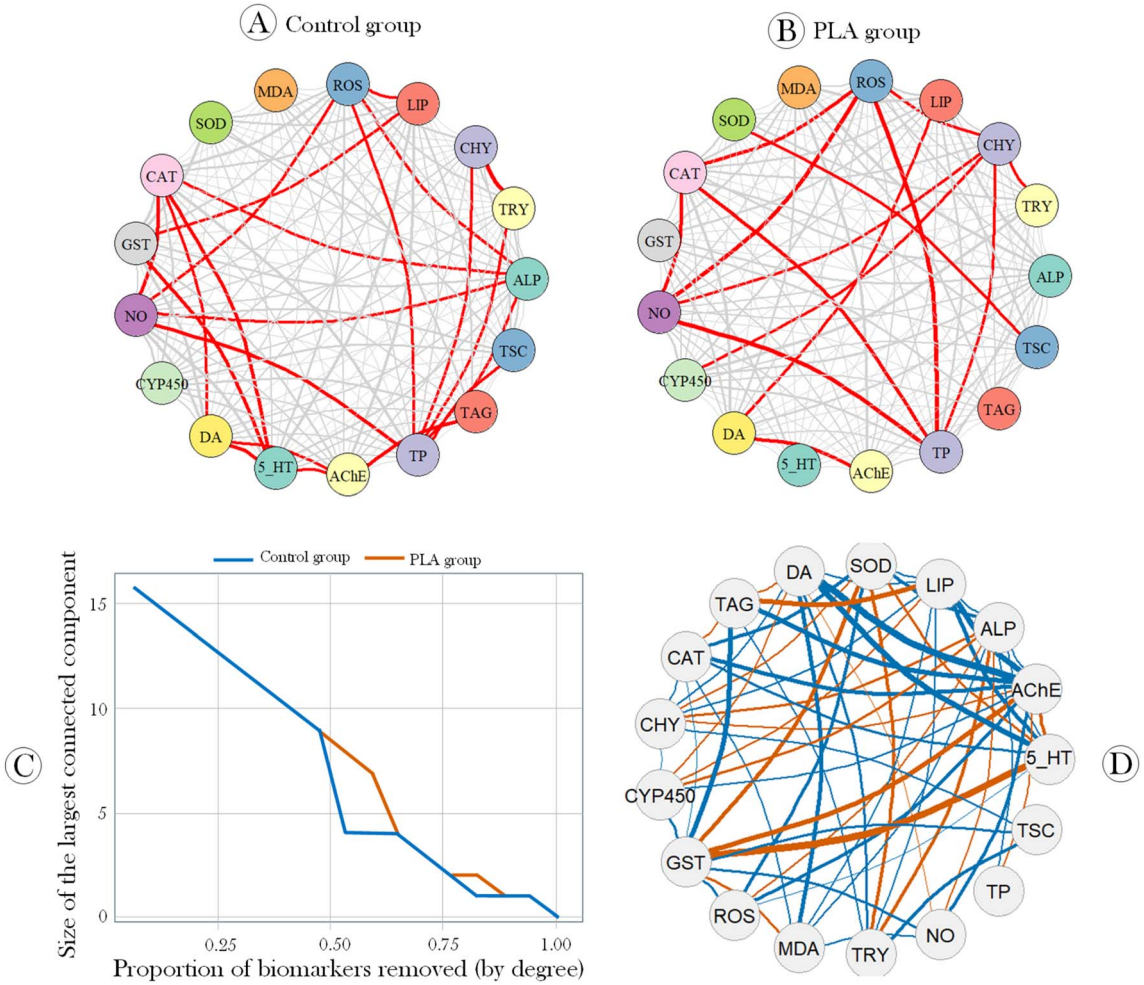

Fig. 3 Functional connectivity analysis of systemic biochemical networks in *Tenebrio molitor* larvae following trophic exposure to polylactic acid microplastics (PLA-MPs). (A and B) Biochemical networks for the control group (A) and PLA-MP-exposed group (B), constructed based on Spearman's correlations between multiple biomarkers. Strong positive correlations ($\rho > 0.7$, $p < 0.05$) are highlighted in red. (C) Network robustness analysis comparing the cumulative node removal impact on connectivity loss for each group. (D) Differential network showing the biochemical interaction shifts between control and PLA-MP groups. Orange edges represent correlations that emerged or were strengthened after PLA-MP exposure (*i.e.*, gained connections). In contrast, blue edges indicate correlations that were lost or weakened (*i.e.*, disappeared from the control network). Each node represents a biochemical biomarker, with abbreviations detailed in the main text. C: control group; PLA: PLA-MP-exposed group. Node labels correspond to biomarkers assessed in Fig. S5 and S6, see "SI". Abbreviations: TP: total protein; TAG: triglycerides; TSC: total soluble carbohydrates; DA: dopamine; 5-HT: serotonin; NO: nitrite; AChE: acetylcholinesterase; CYP450: cytochrome P450-type oxidase; GST: glutathione S-transferase; SOD: superoxide dismutase; CAT: catalase; ROS: reactive oxygen species; MDA: malondialdehyde; TRY: trypsin; CHY: chymotrypsin; LIP: lipase; ALP: alkaline phosphatase.

as 5-HT (degree: 12 → 2), triglycerides (8 → 5), and SOD (6 → 3), while MDA, catalase, and ALP increased their topological influence in the network (Table S3 – see "SI"). In parallel, betweenness centrality analysis highlighted the drastic loss of functional prominence of 5-HT (0.025 → 0.001), suggesting that information flow mediated by this neurotransmitter was severely compromised.

Furthermore, the assessment of network functional resilience revealed striking differences in structural stability between experimental groups. As illustrated in Fig. 3C, the control group's network exhibited greater robustness under the sequential removal of highly connected biomarkers, maintaining a substantially larger connected component throughout the functional collapse curve. In contrast, the PLA group's network showed an abrupt reduction in the size of the largest connected component after approximately 50% of the biomarkers were removed, indicating lower topological resilience and greater functional vulnerability to targeted perturbations. This structural fragility was further corroborated by the differential network analysis (Fig. 3D), which revealed significant changes in biochemical interactions induced by PLA exposure. Connections that disappeared or weakened in the PLA group (shown in orange) represent losses of functional co-activity previously present in control animals. In contrast, interactions that emerged or were intensified in response to PLA (shown in teal blue) suggest compensatory adaptations and a functional reconfiguration of the biochemical system.

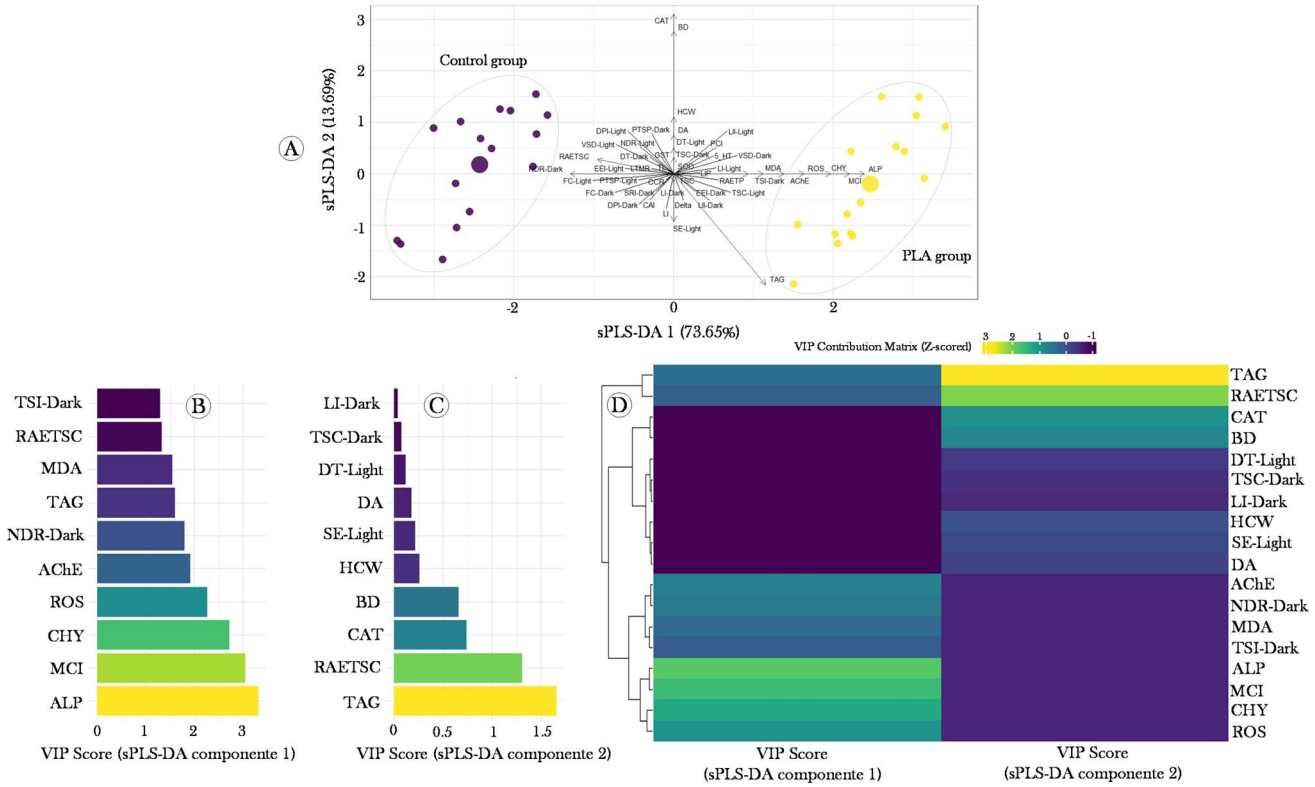

Fig. 4 Integrative multivariate analysis of biochemical, morphometric, and behavioral traits in *Tenebrio molitor* larvae following trophic exposure to polylactic acid microplastics (PLA-MPs). (A) Score plot of the sparse Partial Least Squares-Discriminant Analysis (sPLS-DA), showing clear separation between PLA-exposed and control groups based on the integrated biomarker profile. (B and C) Top 10 variables with the highest discriminative power contributing to the separation along components 1 and 2, respectively. (D) Hierarchical clustering heatmap of *z*-scored values across all traits, illustrating group-specific patterns of response. Color gradients represent relative expression levels (*z*-scores), with yellow indicating higher and purple indicating lower values. The abbreviations used for each variable are explained in Tables S1 and S2.

Finally, to integrate and refine the multivariate discrimination of *T. molitor* larvae fed with PLA-MP-exposed or unexposed flies, we used a supervised modeling approach, sparse Partial Least Squares Discriminant Analysis (sPLS-DA). From a set of 48 independent biomarkers – previously selected through collinearity filtering – the model was fitted with two latent components, which together explained 84.73% of the total variance (73.65% in component 1 and 11.08% in component 2). The clear separation between groups in the projected space (Fig. 4A), combined with the strong vector contribution of biomarkers directed toward the PLA group, confirms the multisystemic effects previously identified in the univariate and discriminant analyses. Evaluation of VIP scores for both components (Fig. 4B and C) revealed that the main discriminants in component 1 (which accounted for the largest variance proportion) were biomarkers associated with bioenergetic reserve capacity [triglyceride levels (TAG) and the Relative Allocation of Energy to Triglycerides index (RAETAG)], digestive enzyme activity [chymotrypsin (CHY) and alkaline phosphatase (ALP)], oxidative stress (ROS and MDA levels, and catalase activity), cholinergic neuroactivity (AChE activity), biophysical body condition [inferred from the Mass Conversion Index (MCI)], and motor and exploratory behavior [represented by the number of direction reversals (NDR) and time spent immobile (TSI), both measured during the dark phase of the behavioral test] (Fig. 4B). Additionally, the subsequent hierarchical clustering of VIPs (Fig. 4D) revealed two major functional clusters with contrasting signatures, suggesting distinct mechanisms of coactivation and functional modularity.

4. Discussion

As recently highlighted by Thompson *et al.*,[1] research on microplastics (MPs) has advanced significantly over recent decades, encompassing analytical, toxicological, ecological, and even socioeconomic dimensions. Nevertheless, despite this progress, critical knowledge gaps persist, particularly in terrestrial ecotoxicology, where information on trophic dynamics involving biodegradable polymers remains scarce. Most studies continue to focus on petroleum-derived MPs in aquatic environments,[42–44] while terrestrial ecosystems and the potential effects of biopolymers such as PLA have been largely overlooked. In this context, the present study offers a novel contribution by investigating the trophic transfer of PLA-MPs between two terrestrial invertebrates – *M. domestica* and *T. molitor* – through an integrated analysis of behavioral, morphometric, biochemical, and functional endpoints. The findings enhance our understanding of the fate, retention

mechanisms, and effects of PLA-MPs across terrestrial trophic chains, providing a foundation for broader discussions on the true ecotoxicological potential of these materials in natural systems.

Initially, the detection of PLA-MPs in newly emerged *M. domestica* adults (Fig. 1A, C and D) confirms their ingestion and retention throughout larval development, as well as their subsequent transfer into the adult stage. This finding suggests that PLA-MPs resist digestion and the intense morphophysiological restructuring that occurs during metamorphosis, a phenomenon also reported in other invertebrates exposed to PLA-MPs [*e.g.*, *Chrysomya megacephala*[35]] or petroleum-derived MPs (*e.g.*, *Aedes aegypti*,[68] *Culex quinquefasciatus*,[69] and *Anopheles* sp.[70]). Furthermore, when offered as food, the contaminated flies mediated the trophic transfer of MPs to *T. molitor* larvae, in which particle accumulation was also observed. The lower concentration and reduced particle diameter in these larvae (Fig. 1A and B) suggest active modification of the polymeric material, possibly partial biodegradation mediated by gut microbiota interactions, consistent with the previously demonstrated capacity of *T. molitor* larvae to degrade various petroleum-based polymers.[71–77] Importantly, the number of particles detected in *T. molitor* larvae should be interpreted as the retained/recovered fraction at the end of the exposure period, rather than as the cumulative number of particles ingested during the five-day feeding period. Therefore, the lower recovered particle burden relative to the estimated particle load available in contaminated flies may indicate that a substantial fraction of PLA-MPs was eliminated through feces, fragmented during gut passage, partially degraded or biotransformed by digestive processes and gut microbiota, or became less detectable after intestinal processing. Additionally, the reduced concentration of PLA-MPs in larvae relative to the initial load observed in flies further supports this hypothesis, aligning with the findings of Peng *et al.*,[78] who showed that PLA can be biodegraded and used as a source of energy and carbon by *T. molitor* larvae. However, because frass, gut contents, and tissues were not analyzed separately, the present study cannot determine the relative contribution of egestion, fragmentation, and partial degradation to the lower recovery of PLA-MPs in *T. molitor* larvae.

On the other hand, this biodegradative ability appears to be accompanied by adverse systemic effects, reflected in multivariate alterations indicative of neurobehavioral dysfunction and disruption of the organism's functional organization. In the behavioral domain, we observed changes in locomotor activity dynamics under both basal conditions (dark section) and aversive stimulation (light section), indicating dysregulation of motor responsiveness. In the open field test, reductions in the number of direction reversals (Fig. S2C), increases in total immobility time (Fig. S1D), and elevated spatial recurrence index (Fig. S2A) suggest decreased locomotor flexibility and exploratory variability. These patterns are consistent with behavioral apathy, lethargy, and possible impairment of attentional motor regulation induced by PLA-MP ingestion. This is similar to behavioral dysfunctions described in other terrestrial macroinvertebrate models exposed to petroleum-based plastic particles, such as *Apis mellifera*,[79] *Drosophila melanogaster*,[80–83] *Bombyx mori*,[84] and *Tribolium castaneum*.[85] Specifically, during the dark phase, the significant reductions in spatial entropy (Fig. S2D) and fractal complexity (Fig. S2E) suggest a more predictable, rigid, and stereotyped exploratory pattern, possibly related to limitations in adaptive strategies under low sensory stimulation. Under intense illumination, the decrease in total distance traveled (Fig. S1A) and in the efficient exploration index (Fig. S2G) observed in PLA-exposed larvae further supports the hypothesis of hyporeactivity to aversive stimuli and impairments in efficient, adaptive environmental exploration.

However, these results contrast with those reported by Silva *et al.*,[86] who observed increased locomotor activity in *Chironomus riparius* larvae exposed to polyurethane MPs, attributing this effect to reduced body mass, which would facilitate movement, and increased AChE activity, interpreted as a reflection of intensified peristaltic movements to expel MPs. In our study, although *T. molitor* larvae exposed to PLA-MPs also showed lower biomass gain (Fig. S3D) and elevated AChE activity (Fig. S6F), the concurrent reduction in dopamine and 5-HT levels (Fig. S6D and E), alongside increased ROS, MDA, and NO levels (Fig. S7E, F and S8C), points to an adverse neurophysiological environment that compromises not only motricity but also motivation and environmental responsiveness. The reduction of these neurotransmitters has been widely associated with motor coordination deficits, apathy, and lethargy, as demonstrated in *Drosophila melanogaster*[87,88] exposed to MPs. Meanwhile, the redox imbalance observed may be linked to multiple mechanisms triggered during PLA biodegradation.

The hyperactivation of digestive enzymes, especially proteases (trypsin and chymotrypsin) and lipase (Fig. S7A–D), may have increased energy expenditure and intensified mitochondrial activity for enzyme synthesis and function, resulting in higher ROS generation as metabolic by-products, exacerbated by the concurrent reduction in antioxidant defenses (SOD and catalase; Fig. S7G and H). As highlighted by Shalem *et al.*,[23] these enzymes may have acted not only on dietary proteins and lipids (from contaminated flies) but also on the ingested PLA itself, given its ester bonds. Previous studies suggest that alkaline serine proteases (such as those found in insects) can hydrolyze PLA, particularly the poly-L-lactic acid and poly-D,L-lactic acid forms,[89,90] which may also apply to lipases adapted to polyester degradation. Moreover, enzymatic action on PLA-protein or PLA-lipid complexes could have generated digestively active hybrids, further intensifying intestinal enzymatic activity. This functional overload likely led to intracellular ROS accumulation, contributing to increased lipid peroxidation, as reflected by elevated MDA levels (Fig. S5F). Additionally, the activation of phase I enzymes, such as CYP450-type oxidases (Fig. S6B), without compensatory GST upregulation (Fig. S6A), suggests an imbalance in detoxification pathways, potentially leading to the accumulation of reactive intermediates. It is also plausible that redox imbalance was amplified by genomic mechanisms, such as the induction of degradative genes involved in plastic metabolism, as suggested by Peng *et al.*[49] in *T. molitor* larvae exposed to PVC, PS, and PLA.

Furthermore, our data indicate a decisive metabolic contribution to the behavioral dysfunctions observed, suggesting that bioenergetic alterations underpin the neurobehavioral responses induced by PLA-MPs. Evidence of energy depletion – such as the significant reduction in total protein and soluble carbohydrate levels (Fig. S4A and S6C) – points to limited structural reserves and rapidly mobilizable energy resources, which are essential for sustaining locomotor activity and immediate adaptive responses. In parallel, the increase in triglyceride levels (Fig. S4B) and in the Relative Allocation of Energy to Triglycerides index (RAETAG; Fig. S4E) reveals a metabolic reorientation favoring long-term energy storage at the expense of metabolic readiness, as indicated by the reduction in the Rapid Energy Allocation Index (REAI; Fig. S4G). This pattern contrasts with that observed by Silva *et al.*,[86] where the increase in energy allocated to locomotion in *C. riparius* larvae occurred at the expense of somatic growth. In contrast, our study found that metabolic prioritization appeared to favor passive energy retention, thereby impairing behavioral responsiveness. This redistribution, combined with the reduced allocation to proteins (RAETP; Fig. S4D), reflects an unfavorable physiological state that prioritizes energy accumulation over structural and behavioral functions, directly impacting locomotor flexibility and responsiveness to environmental stimuli. This interpretation is further supported by biometric data, which reveal ontogenetic delay (larval instar; Fig. S3A), lower biomass gain (Fig. S3D), and an increase in the Mass Conversion Index (MCI; Fig. S3E), the latter indicating higher energetic cost for converting cephalic volume into functional biomass, characterizing an inefficient growth profile under metabolic stress.

From an integrative perspective, our results indicate that exposure to PLA-MPs significantly disrupted the functional architecture of the systemic biochemical network, inducing a structural reorganization marked by the loss of functional connections (degree) among key biomarkers such as SOD and AChE activity, and levels of 5-HT and triglycerides [Fig. 3 and Table S3 (see "SI")]. This breakdown in connectivity suggests a progressive collapse in the functional integration of the serotonergic, antioxidant, lipidic, and neurochemical axes. In contrast, biomarkers such as catalase, GST, trypsin, MDA, and nitrite assumed more central functional positions, indicating a redirection of systemic interactions toward pathways associated with oxidative stress, inflammation, and terminal metabolism. Notably, MDA emerged as a node with high betweenness, despite its peripheral role in the control network, highlighting its increased functional relevance in larvae fed contaminated flies and reflecting the dominance of degenerative processes mediated by lipid peroxidation. Similarly, the increase in betweenness for catalase and GST suggests the activation of compensatory mechanisms in response to oxidative stress, although these appear insufficient to restore redox homeostasis. These findings, combined with results from supervised multivariate modeling (sPLS-DA), support the hypothesis that exposure to PLA-MPs promotes a coordinated, multisystemic phenotypic reorganization capable of discriminating between experimental groups based on complex functional signatures (Fig. 4). Such evidence advances the field beyond most microplastic ecotoxicity studies, which often rely on isolated biomarker analysis. By integrating multiple variables through co-occurrence networks and discriminant modeling, our data reveal emergent alterations in interdependent functional relationships that conventional univariate approaches would not detect. Although the scarcity of studies focused on the integrative ecotoxicology of PLA-MPs limits direct comparisons, our findings converge with those of Liao *et al.*,[91] who reported reduced structural robustness in the gut microbial networks of *Oryzias melastigma* exposed to polystyrene MPs and tetracycline, and with Guimarães *et al.*,[35] who observed functional disorganization in *C. megacephala* exposed to PS-MPs, evidenced by negative correlations and disconnected patterns among oxidative and neurochemical biomarkers.

In this context, the findings presented here demonstrate that PLA-MPs, despite their "biodegradable" labeling, can trigger adverse multisystemic effects even after a single trophic transfer step, impairing behavioral performance, ontogenetic development, and bioenergetic metabolism in *T. molitor* larvae. Considering the crucial ecological role of *T. molitor* as a detritivore with broad dietary capacity – including the consumption of both plant- and animal-derived materials[92,93] – such dysfunctions may directly impact organic matter decomposition efficiency, nutrient cycling, and the structure of soil food webs. In natural environments and agroecosystems, where *T. molitor* or functionally analogous species serve as a link between detrital resources and higher-order consumers, the disruption of these processes could promote broad ecological imbalances, affecting everything from soil renewal to energy availability at higher trophic levels. Furthermore, the data reinforce previous studies warning that the mere classification of a polymer as "biodegradable" does not ensure environmental safety, particularly when introduced into biological systems that do not replicate the ideal conditions for its safe degradation.[94–96] Taken together, our findings underscore the urgency of incorporating the ecotoxicological and trophic implications of biodegradable plastics into environmental/ecological risk assessments, especially in scenarios where indirect exposure *via* predation constitutes a plausible route of contamination and bioaccumulation.

5. Limitations and future perspectives

Although our study represents a methodological and conceptual advance in evaluating the trophic transfer of biodegradable MPs in terrestrial ecosystems, several limitations should be acknowledged to guide future research. Among its main innovations, the study realistically simulated a detritivore food chain using ecologically relevant species and applied a multisystemic biomarker panel capable of detecting behavioral, biometric, and biochemical alterations induced by a single predation step. Still, our experimental design included only one PLA-MP concentration, which had been previously classified as environmentally plausible. While this choice ensures ecological relevance, the lack of an exposure gradient limits the ability to characterize dose–response relationships and determine

potential effect thresholds. Additionally, although the use of Nile Red-stained fluorescent particles and their detection *via* epifluorescence microscopy strengthened the identification of PLA-MPs at both trophic levels, future assessments that distinguish anatomical compartments (*e.g.*, digestive tract *vs.* tissues) and investigate secondary fragmentation along the digestive tract may provide more robust insights into systemic bioavailability and particle metabolism.

Another limitation lies in the choice of a single prey–predator interaction (*M. domestica* → *T. molitor*), which, although ecologically grounded, restricts the extrapolation of findings to more complex trophic chains or organisms from different trophic guilds. Moreover, ecotoxicological effects were evaluated only after a short exposure period (five days), which may underestimate cumulative impacts, compensatory alterations, or delayed effects. At the biochemical level, despite the application of a comprehensive set of functional biomarkers, including digestive activity, redox parameters, neurotransmitters, and energy reserves, future studies incorporating molecular analyses (*e.g.*, gene expression) or reproductive markers will enhance our understanding of causal mechanisms and potential population-level consequences.

Thus, future perspectives include incorporating multiple trophic levels and functionally distinct species, testing different concentrations and types of biodegradable polymers [*e.g.*, poly(succinic acid) (PSA), poly(butylene adipate-*co*-terephthalate) (PBAT), polyhydroxybutyrate (PHB), and poly(-caprolactone) (PCL)], and expanding endpoints to include potential histopathological damage, stress-related gene expression, reproduction, and immunocompetence. The application of advanced imaging tools (*e.g.*, confocal microscopy, Raman mapping, or micro-CT) could contribute to more precise particle tracking in tissues and elucidation of biodistribution.[97–99] Finally, studies in microcosms or under controlled edaphic conditions that integrate multiple environmental factors (pH, temperature, microbiota, and organic matter) may provide greater ecological realism and aid in the external validation of our laboratory findings, ultimately contributing to the refinement of predictive environmental risk models associated with biopolymers.

6. Conclusion

In conclusion, our study demonstrated that PLA-MPs can be effectively transferred along the evaluated terrestrial food chain (*M. domestica* → *T. molitor*), even in the absence of direct environmental exposure, and that this transfer is capable of inducing locomotor disorganization, ontogenetic impairment, and functional collapse across multiple physiological systems in the predator organism (*T. molitor* larvae). The central hypothesis – that PLA-MPs, despite being labeled as biodegradable, hold significant ecotoxicological potential when conveyed through contaminated prey – was confirmed through multiple lines of evidence, including fluorescence-detected indirect bioaccumulation, vector-based behavioral alterations, and functional network complexity loss. By applying an analytical framework that integrates supervised learning (PLS-DA and sPLS-DA), unsupervised dimensionality reduction (PCA), and functional connectivity inference (complex network analysis) within an ecologically valid trophic model, our study enabled the characterization of integrated ecotoxicological disturbance signatures in multicompartment biological systems. More than raising concerns about the use of biodegradable plastics, the findings presented here underscore the need for critical revisions to regulatory assumptions and environmental risk assessment methodologies for emerging materials. From this point forward, new questions arise: which classes of biopolymers share this potential for indirect toxicity? How do these dysfunctions manifest in more complex ecological interactions over time? And what are the implications for organic matter decomposition and soil ecosystem functioning? By addressing these questions, the ecotoxicology of biopolymers can move toward more holistic, ecologically grounded, and functionally integrated approaches.

Ethical approval

Although this study did not involve the use of vertebrate animals and is therefore not subject to mandatory review by an Institutional Animal Care and Use Committee (IACUC) or an equivalent ethics board, all procedures were conducted in accordance with internationally recognized standards for the ethical treatment of invertebrates in scientific research. The experimental design followed the 3Rs principles (Replacement, Reduction, and Refinement) to minimize potential distress and ensure responsible animal handling. All efforts were made to reduce unnecessary manipulation and to maintain optimal environmental and husbandry conditions throughout the experimental period.

Author contributions

Bruna de Oliveira Mendes: conceptualization, methodology, investigation, validation, visualization, writing – original draft, and writing – review & editing. Wesley Rodrigues Soares, Rafaela Ribeiro de Brito, Ariane Guimarães, and Thiarlen Marinho da Luz: conceptualization, methodology, investigation, validation, visualization, and writing – review & editing. Aline Sueli de Lima Rodrigues and Boscolli Barbosa Pereira: validation, visualization, and writing – review & editing. Guilherme Malafaia: conceptualization, methodology, validation, formal analysis, resources, data curation, writing – original draft, review and editing, supervision, project administration, funding acquisition.

Conflicts of interest

We confirm that there are no known conflicts of interest associated with this work, and that there has been no significant financial support that could have influenced its outcome. All listed authors have thoroughly read and approved the manuscript, and no other individuals meet the authorship criteria but are omitted. We emphasize that the peer review process is entirely under the responsibility of the handling editor, who has

full autonomy to select, invite, and assign qualified reviewers based on their scientific expertise and relevance to the topic. The editor also retains exclusive authority over all editorial decisions related to the manuscript's evaluation and potential publication. We reaffirm our commitment to upholding the highest ethical standards in scientific publishing and to ensuring an impartial, transparent, and rigorous review process.

Data availability

All data generated or analyzed during this study are included in this published article. Furthermore, the data supporting this study's findings are available on request from the corresponding author, [Malafaia G.].

Supplementary information (SI) is available. See DOI: https://doi.org/10.1039/d6va00175k.

Acknowledgements

The authors thank the National Council for Scientific and Technological Development (CNPq/Brazil) for the financial support provided for the development of this research and for the productivity fellowship awarded to the corresponding author (Malafaia, G.) (process no. 308854/2021-7), whose support was fundamental for the successful execution of this study. In addition, we also acknowledge the Coordination for the Improvement of Higher Education Personnel (CAPES/Brazil) for the doctoral scholarship granted to the first author (Mendes, B. O.).

In this study, we utilized artificial intelligence tools, specifically GPT-5.5, developed by OpenAI and accessed through the OpenAI platform. The GPT-5.5 version was employed for linguistic enhancement and data processing, providing guidance on the necessary transformations to adapt the data and suggesting which statistical analyses would be most suitable to achieve the study's objectives. We ensured that the AI tool was used under strict human supervision, guaranteeing the accuracy and integrity of the results. This statement reflects our commitment to transparency and methodological rigor, ensuring that the integration and validation of AI use were adequately managed throughout all stages of the research.

References

1 R. C. Thompson, W. Courtene-Jones, J. Boucher, S. Pahl, K. Raubenheimer and A. A. Koelmans, *Science*, 2024, **386**, eadl2746.
2 R. Debnath, G. S. Prasad, A. Amin, M. M. Malik, I. Ahmad, A. Abubakr, *et al.*, *J. Contam. Hydrol.*, 2024, **266**, 104399.
3 K. B. Megha, D. Anvitha, S. Parvathi, A. Neeraj, J. Sonia and P. V. Mohanan, *Crit. Rev. Biotechnol.*, 2025, **45**, 97–127.
4 D. Kim, S. A. Kim, S. H. Nam, J. I. Kwak, L. Kim, T. Y. Lee, *et al.*, *Mar. Pollut. Bull.*, 2024, **200**, 116056.
5 S. Gao, X. Mu, W. Li, Y. Wen, Z. Ma, K. Liu and C. Zhang, *Environ. Geochem. Health*, 2025, **47**, 158.
6 T. Ahmad, S. Gul, L. Peng, T. Mehmood, Q. Huang, A. Ahmad, *et al.*, *Environ. Chem. Lett.*, 2025, 1–26.
7 V. H. Hoang, M. K. Nguyen, T. D. Hoang, N. Rangel-Buitrago, C. Lin, M. T. Pham, *et al.*, *Environ. Chem. Lett.*, 2025, 1–21.
8 S. Padha, R. Kumar, A. Dhar and P. Sharma, *Environ. Res.*, 2022, **207**, 112232.
9 A. Benito-Kaesbach, J. Suárez-Moncada, A. Velastegui, J. Moreno-Mendoza, M. Vera-Zambrano, U. Avendaño, *et al.*, *Environ. Pollut.*, 2024, **347**, 123772.
10 J. P. Frias and R. Nash, *Mar. Pollut. Bull.*, 2019, **138**, 145–147.
11 J. Song, C. Wang and G. Li, *ACS ES&T Water*, 2024, **4**, 2330–2332.
12 P. Liu, X. Zhan, X. Wu, J. Li, H. Wang and S. Gao, *Chemosphere*, 2020, **242**, 125193.
13 Y. Li, W. Ling, C. Hou, J. Yang, Y. Xing, Q. Lu, *et al.*, *J. Hazard. Mater.*, 2025, 137977.
14 W. Li and F. Meng, *Mar. Pollut. Bull.*, 2025, **214**, 117758.
15 S. Ghosh, S. Dey, A. H. Mandal, A. Sadhu, N. C. Saha, D. Barceló, *et al.*, *J. Contam. Hydrol.*, 2025, 104514.
16 C. Gao, B. Xu, Z. Li, Z. Wang, S. Huang, Z. Jiang, *et al.*, *Aquat. Toxicol.*, 2025, 107242.
17 H. S. Samuel, F. D. M. Ekpan and M. O. Ori, *Asian J. Environ. Res.*, 2024, **1**, 152–165.
18 S. Rajendran, A. Al-Samydai, G. Palani, H. Trilaksana, T. Sathish, J. Giri, *et al.*, *Eng. Rep.*, 2025, **7**, e70108.
19 S. Dubey, K. Sharma, B. Raikwar and S. Mishra, in *Polyhydroxyalkanoates: Sustainable Production and Biotechnological Applications II: Agriculture, Industry, and Environment*, Springer Nature Singapore, Singapore, 2025, pp. 13–39.
20 C. Lors, P. Leleux and C. H. Park, *Front. Mater.*, 2025, **11**, 1476484.
21 L. Ranakoti, B. Gangil, S. K. Mishra, T. Singh, S. Sharma, R. A. Ilyas and S. El-Khatib, *Materials*, 2022, **15**, 4312.
22 N. Shekhar and A. Mondal, *Polym. Bull.*, 2024, **81**, 11421–11457.
23 A. Shalem, O. Yehezkeli and A. Fishman, *Appl. Microbiol. Biotechnol.*, 2024, **108**, 413.
24 R. Kaur and I. Chauhan, *Biodegradation*, 2024, **35**, 863–892.
25 L. Han, L. Chen, Y. Feng, Y. Kuzyakov, Q. A. Chen, S. Zhang, *et al.*, *Environ. Int.*, 2024, **185**, 108508.
26 R. Liu, J. Liang, Y. Yang, H. Jiang and X. Tian, *Chemosphere*, 2023, **329**, 138504.
27 Y. Lian, W. Liu, R. Shi, A. Zeb, Q. Wang, J. Li, *et al.*, *J. Hazard. Mater.*, 2022, **435**, 129057.
28 S. Bao, X. Wang, J. Zeng, L. Yue, Z. Xiao, F. Chen and Z. Wang, *Front. Plant Sci.*, 2025, **16**, 1544298.
29 Y. Han, M. Fu, J. Wu, S. Zhou, Z. Qiao, C. Peng, *et al.*, *Sci. Total Environ.*, 2023, **862**, 160909.
30 E. Liwarska-Bizukojc, P. Bernat and A. Jasińska, *Sci. Total Environ.*, 2023, **898**, 165423.
31 M. Parolini, B. De Felice, S. Gazzotti, M. Sugni and M. A. Ortenzi, *Environ. Pollut.*, 2024, **348**, 123868.
32 L. E. Castelli, R. M. Gleiser and M. Battán-Horenstein, *Ecol. Entomol.*, 2020, **45**, 718–726.
33 A. P. Paliy, N. V. Sumakova and K. V. Ishchenko, *Ukr. J. Ecol.*, 2018, **8**, 230–234.

34 M. D. Finke and D. Oonincx, in *Mass Production of Beneficial Organisms*, Academic Press, 2023, pp. 511–540.
35 A. Guimarães, A. T. B. Guimarães, R. R. de Brito, A. R. Gomes, Í. N. Freitas, A. S. de Lima Rodrigues, *et al.*, *Arch. Environ. Contam. Toxicol.*, 2025, 1–20.
36 S. Lievens, E. Vervoort, D. Bruno, T. Van der Donck, G. Tettamanti, J. W. Seo, *et al.*, *Sci. Rep.*, 2023, **13**, 4341.
37 E. Demir, *J. Toxicol. Environ. Health, Part A*, 2021, **84**, 649–660.
38 F. Turna-Demir, G. Akkoyunlu and E. Demir, *Biology*, 2022, **11**, 1470.
39 M. Abdulla, J. C. Barnes, O. M. Poole, K. R. Wotton and E. Jimenez-Guri, *Microplastics*, 2025, **4**, 22.
40 S. Saikumar, R. Mani, M. Ganesan, I. Dhinakarasamy, T. Palanisami and D. Gopal, *J. Hazard. Mater.*, 2024, **464**, 132927.
41 S. S. Singh, R. Chanda, N. S. Singh, Ramtharmawi, N. R. Devi, K. V. Devi, *et al.*, *Discover Environ.*, 2024, **2**, 103.
42 M. Zhang, Y. Jin, C. Fan, Y. Xu, J. Li, W. Pan, *et al.*, *Environ. Pollut.*, 2024, **357**, 124426.
43 S. Gao, Z. Li and S. Zhang, *Mar. Pollut. Bull.*, 2024, **200**, 116082.
44 Y. F. Ma and X. Y. You, *Aquaculture*, 2025, **594**, 741463.
45 E. H. Lwanga, J. M. Vega, V. K. Quej, J. D. Chi, L. S. Del Cid, C. Chi, *et al.*, *Sci. Rep.*, 2017, **7**, 14071.
46 Y. Chae and Y. J. An, *Environ. Sci.: Nano*, 2020, **7**, 975–983.
47 H. Sanchez-Arroyo and J. L. Capinera, *IFAS Extension-University of Florida*, 2017.
48 K. D. Ileke, M. F. Olaoye and I. O. Olabimi, *Leban. Sci. J.*, 2020, **21**, 146.
49 B. Y. Peng, Y. Sun, P. Li, S. Yu, Y. Xu, J. Chen, *et al.*, *J. Environ. Manage.*, 2023, **345**, 118818.
50 M. Q. Ding, J. Ding, Z. R. Zhang, M. X. Li, C. H. Cui, J. W. Pang, *et al.*, *J. Environ. Manage.*, 2024, **358**, 120832.
51 I. Vital-Vilchis and E. Karunakaran, *Insects*, 2025, **16**, 165.
52 X. Wang, R. Du, F. N. Henriquez, H. Liu, S. Y. Chan, C. M. Leong and M. Y. Lui, *Adv. Energy Sustainability Res.*, 2025, 2400378.
53 A. Babczyńska, M. Bańska, K. Mizera, M. Tarnawska, M. Augustyniak, K. Rozpędek, *et al.*, *Ecotoxicol. Environ. Saf.*, 2025, **298**, 118289.
54 A. Naccarato, M. L. Vommaro, R. Elliani, A. Babczyńska, A. Tagarelli and A. Giglio, *J. Hazard. Mater.*, 2025, **494**, 138556.
55 A. Brai, F. Poggialini, C. Vagaggini, C. Pasqualini, S. Simoni, V. Francardi and E. Dreassi, *Int. J. Mol. Sci.*, 2023, **24**, 2296.
56 L. L. V. De-Mello-Braga, G. Simão, C. S. Schiebel, Y. F. Oliveira, L. B. da Rosa, M. B. Gois, *et al.*, *Pharmacol. Res.*, 2024, **2**, 100013.
57 C. Adamaki-Sotiraki, C. I. Rumbos and C. G. Athanassiou, *J. Pest Sci.*, 2025, **98**, 113–129.
58 M. A. Mahmoud, A. O. Abotaleb and R. A. Zinhoum, *Sci. Rep.*, 2025, **15**, 1.
59 A. P. C. Araújo, N. F. S. de Melo, A. G. de Oliveira Junior, F. P. Rodrigues, T. Fernandes, J. E. de Andrade Vieira, *et al.*, *J. Hazard. Mater.*, 2020, **382**, 121066.
60 R. W. Crosskey and R. P. Lane, in *Medical Insects and Arachnids*, Springer Netherlands, Dordrecht, 1993, pp. 403–428.
61 C. J. Geden, D. Nayduch, J. G. Scott, E. R. Burgess IV, A. C. Gerry, P. E. Kaufman, *et al.*, *J. Integr. Pest Manage.*, 2021, **12**, 39.
62 M. Bläsing and W. Amelung, *Sci. Total Environ.*, 2018, **612**, 422–435.
63 R. O. Ferreira, A. T. B. Guimarães, T. M. da Luz, A. S. de Lima Rodrigues, A. R. M. T. Islam, M. M. Rahman, *et al.*, *Sci. Total Environ.*, 2023, **882**, 163617.
64 M. Janković-Tomanić, B. Petković, J. S. Vranković and V. Perić-Mataruga, *J. Insect Sci.*, 2024, **24**, 6.
65 C. E. Balfour and L. Carmichael, *Am. J. Psychol.*, 1928, **40**, 576–584.
66 D. J. McLean and M. A. Skowron Volponi, *Ethology*, 2018, **124**, 440–448.
67 J. A. Morales-Ramos, S. Kay, M. G. Rojas, D. I. Shapiro-Ilan and W. L. Tedders, *Ann. Entomol. Soc. Am.*, 2015, **108**, 146–159.
68 A. Simakova, A. Varenitsina, I. Babkina, Y. Andreeva, R. Bagirov, V. Yartsev and Y. Frank, *Water*, 2022, **14**, 1852.
69 J. H. Li, X. H. Liu, G. R. Liang, H. T. Gao, S. H. Guo, X. Y. Zhou, *et al.*, *Sci. Total Environ.*, 2024, **917**, 170547.
70 A. V. Simakova, A. A. Varenitsina, I. B. Babkina, Y. V. Andreeva and Y. A. Frank, *Entomol. Exp. Appl.*, 2024, **172**, 1046–1053.
71 A. M. Brandon, S. H. Gao, R. Tian, D. Ning, S. S. Yang, J. Zhou, *et al.*, *Environ. Sci. Technol.*, 2018, **52**, 6526–6533.
72 B. Y. Peng, Z. Chen, J. Chen, H. Yu, X. Zhou, C. S. Criddle, *et al.*, *Environ. Int.*, 2020, **145**, 106106.
73 W. M. Wu and C. S. Criddle, in *Methods in Enzymology*, Academic Press, 2021, vol. 648, pp. 95–120.
74 Y. Lou, Y. Li, B. Lu, Q. Liu, S. S. Yang, B. Liu, *et al.*, *J. Hazard. Mater.*, 2021, **416**, 126222.
75 T. Mamtimin, H. Han, A. Khan, P. Feng, Q. Zhang, X. Ma, *et al.*, *Microbiome*, 2023, **11**, 98.
76 Y. Wang, X. Zhao, J. Wang, Y. Weng, Y. Wang, X. Li and X. Han, *J. Environ. Chem. Eng.*, 2023, **11**, 110801.
77 B. Y. Peng, Y. Xu, X. Zhou, W. M. Wu and Y. Zhang, *Environ. Sci. Technol.*, 2024, **58**, 10368–10377.
78 B. Y. Peng, Z. Chen, J. Chen, X. Zhou, W. M. Wu and Y. Zhang, *J. Hazard. Mater.*, 2021, **416**, 125803.
79 P. Balzani, G. Galeotti, S. Scheggi, A. Masoni, G. Santini and D. Baracchi, *Environ. Pollut.*, 2022, **305**, 119318.
80 Y. Zhang, M. B. Wolosker, Y. Zhao, H. Ren and B. Lemos, *Sci. Total Environ.*, 2020, **744**, 140979.
81 S. Matthews, E. G. Xu, E. R. Dumont, V. Meola, O. Pikuda, R. S. Cheong, *et al.*, *Environ. Sci.: Nano*, 2021, **8**, 110–121.
82 F. Kong, H. Jin, X. Li and J. Shen, *J. Environ. Manage.*, 2024, **370**, 122846.
83 H. Ranjan, S. S. Kumar, S. Priscilla, S. Swaminathan, M. Umezawa and S. S. Mohideen, *Environ. Sci.: Processes Impacts*, 2024, **26**, 2203–2214.
84 C. C. Parenti, A. Binelli, S. Caccia, C. Della Torre, S. Magni, G. Pirovano and M. Casartelli, *Chemosphere*, 2020, **257**, 127203.

85 G. Malafaia, A. Guimarães, W. R. Soares, I. P. P. de Menezes, A. S. de Lima Rodrigues, A. R. Gomes, *et al.*, *Environ. Res.*, 2025, 122462.
86 S. A. Silva, A. C. Rodrigues, T. Rocha-Santos, A. L. P. Silva and C. Gravato, *Int. J. Environ. Res. Public Health*, 2022, **19**, 15610.
87 T. Riemensperger, G. Isabel, H. Coulom, K. Neuser, L. Seugnet, K. Kume, *et al.*, *Proc. Natl. Acad. Sci. U. S. A.*, 2011, **108**, 834–839.
88 T. Riemensperger, A. R. Issa, U. Pech, H. Coulom, M. V. Nguyễn, M. Cassar, *et al.*, *Cell Rep.*, 2013, **5**, 952–960.
89 Y. Tokiwa and B. P. Calabia, *Appl. Microbiol. Biotechnol.*, 2006, **72**, 244–251.
90 Y. Oda, A. Yonetsu, T. Urakami and K. Tonomura, *J. Polym. Environ.*, 2000, **8**, 29–32.
91 X. Liao, P. Zhao, L. Hou, B. Adyari, E. G. Xu, Q. Huang and A. Hu, *J. Hazard. Mater.*, 2023, **442**, 129996.
92 M. S. Rho and K. P. Lee, *J. Insect Physiol.*, 2014, **71**, 37–45.
93 C. I. Rumbos, I. T. Karapanagiotidis, E. Mente, P. Psofakis and C. G. Athanassiou, *Sci. Rep.*, 2020, **10**, 11224.
94 L. Zimmermann, A. Dombrowski, C. Völker and M. Wagner, *Environ. Int.*, 2020, **145**, 106066.
95 M. Alaraby, D. Abass, M. Farre, A. Hernández and R. Marcos, *Sci. Total Environ.*, 2024, **919**, 170592.
96 A. Das, S. Mishra and B. Tripathy, *Innovative Infrastruct. Solutions*, 2025, **10**, 321.
97 A. Benito-Kaesbach, J. M. Amigo, U. Izagirre, N. Garcia-Velasco, L. Arévalo, A. Seifert and K. Castro, *Sci. Total Environ.*, 2023, **876**, 162810.
98 V. Parobková, L. Maleček, M. Zemek, G. Kalčíková, M. Vykypělová, M. Buchtová, *et al.*, *J. Hazard. Mater.*, 2025, **488**, 137442.
99 Y. Umurhan, M. Songsart-Power, T. B. Limbu and T. Phan, *Environ. Sci. Pollut. Res.*, 2025, 1–48.